ADVANCED ELECTROMAGNETICS, Vol. 2, No. 3, December 2013

Fabrication and characterization of micro-inductors deposited on magnetic thin and thick layers

Allassem Désiré[1], Adoum Kriga[1], Mahamoud Youssouf[2], Ali Siblini[1], Jean-Pierre Chatelon[1*], Marie-Françoise Blanc-Mignon[1], Béatrice Payet-Gervy[1], Alain Piot[3], Didier Dufeu[4], Jean-Jacques Rousseau[1*]

[1]Université de Lyon, F-42023, Saint Etienne, France; Université de Saint Etienne, Jean Monnet, F-42023, Saint Etienne, France; LT2C, F-42023, Saint Etienne, France
[2]IUSTA BP 6033 N'Djamena TCHAD
[3]Université de Lyon, F-42023, Saint Etienne, France; Université de Saint Etienne, Jean Monnet, F-42023, Saint Etienne, France; IUT, F-42023, Saint Etienne, Franc
[4]Institut Néel, CNRS/UJF, BP166, 38042 Grenoble-cedex 09, France
*corresponding author, E-mail: chatelon@univ-st-etienne.fr

Abstract

This paper presents two fabrication techniques of spiral integrated inductors based on magnetic materials. For the first one, the magnetic core is a thin film deposited by RF magnetron sputtering, for the second technique the magnetic core is a thick layer of YIG obtained by micromachining. The addition of the magnetic material is expected to improve the performances of the integrated structure with electromagnetic shield. Low and high frequency equipment are used to characterize the manufactured components. A good correlation is obtained between the results by simulation and measurements for the two manufacturing techniques. These results show that the inductance increases when the thickness of the magnetic layer increases, we can double the inductance value for a thickness sufficiently high.

1. Introduction

The interest of the integrated inductors and transformers, based on magnetic materials, is in a continuous evolution in order to reduce the cost and the size of high frequency passive components. They are usually used in: power conversion integrated circuits [1, 2], RF and microwaves passive components [3-10] and wireless communications devices [11, 12].

For the fabrication of such inductors, two manufacturing technologies are generally used: Micro-Electro-Mechanical Systems (MEMS) and Monolithic Microwave Integrated Circuits (MMIC). MEMS fabrication technology is derived largely from microelectronics technique. Substrates of various kinds (particularly silicon) are used; the microsystem is produced by a succession of micro-machining, photolithography and wet or dry etching [9, 11, 13, 14]. In the case of the MMIC technology, the manufacturing process involves depositing a number of successive layers of metals and dielectrics. The patterns of the deposited layers can be done by two different lithographic processes which are lift-off or etching [5, 7, 15].

The fabrication is followed by a characterization permitting to show the performance of the manufactured component. At low frequency, LCR-meters are generally used to measure the impedance of the device under test with RL series model. However, at high frequency, network analyzers are used. The results are deduced from S parameters [14, 15]. These results are often compared with the results of theoretical studies or simulation. The simulators used in the case of inductors are HFSS or Momentum [12, 14, 16, 17].

In this work, we propose the manufacturing processes of micro-integrated planar inductors with two types of magnetic core. The first one is a magnetic thin film of Yttrium Iron Garnet (YIG) deposited by RF magnetron sputtering [18, 19]. The second one is a thick layer of YIG obtained by micromachining of a bulk wafer. The low and high frequency characterizations are performed using two different systems. In order to reduce inductors size and to increase their performance, a magnetic material is used to canalize the field lines. For low frequency, we have used a measurement equipment composed of a LCR-meter HP4284A working from 20 Hz up to 1 MHz and a four-probe test bench. The inductance value L has been simulated and measured for a conducting spiral inductor without and with magnetic material. For thin films of thickness less than 18 μm, L is multiplied by 1.14 and by 2 for thick layers comparing with the inductance of the coreless conducting spiral inductor. We have noticed also that there is a very good correlation between the simulated and the measured values of L.

2. Design of the component

To design the integrated inductor structure, we have used the electromagnetic simulation software HFSS marketed by ANSOFT. This software uses the finite element method. The studied structure is a thin film of copper having the shape of a spiral ribbon. The geometrical characteristics are defined as follows: the number of turns (N), the ribbon width (R), the distance between two consecutive turns (D), the thickness of YIG film (E_{YIG}), the thickness of copper ribbon (E_{Co}) and the substrate thickness (E_{sub}) (Fig. 1 and Fig. 2). After studying different spiral shapes of the coil (square, circular and octagonal) and different number of turns, the design of figure 1 has given the better results [17].

Two types of structures have been studied: a square spiral inductor without magnetic material (Fig.2a) and with YIG layers of different thicknesses (Fig. 2b). To assess the contribution of the magnetic material, experimental and numerical studies are presented and compared. The shape and the dimensions of the mask permitting to manufacture the spiral inductor of figure 1 were obtained using HFSS simulator. For the dimensions, we have chosen $N = 7$, $R = 125$ µm and $D = 60$ µm. The magnetic material (YIG) and the substrate (Al_2O_3) are used in our Laboratory for their interests in radio-frequency and micro-wave fields.

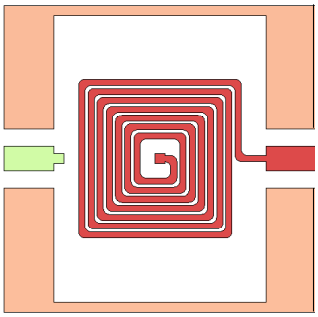

Figure 1: Square spiral inductor with guard plane shielding

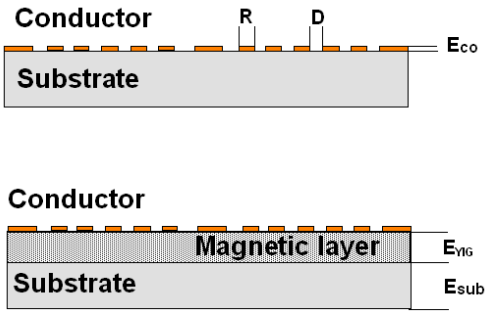

Figure 2: Patterns of spiral inductors with and without magnetic material

3. Fabrication of the integrated inductor with thin magnetic film

In this section, we describe the main steps for the fabrication of an integrated inductor with thin magnetic film obtained by RF sputtering. These steps are performed as follows:

- Deposition of the magnetic layer on the alumina substrate.
- Annealing of the deposited film necessary to obtain a crystalline magnetic material.
- Deposition of the copper film on the magnetic layer.
- Photolithography and wet etching necessary to obtain the pattern of the spiral inductor.
- And finally, the wire bonding for the terminal connections.

3.1. Deposition, annealing and characterization of the magnetic thin film

Magnetic films are deposited on alumina substrate of controlled roughness by RF magnetron sputtering. This technique is well suited for deposition of conductive and insulating material as copper and YIG respectively. The main parameters of the deposition are given in table 1.

Table 1: RF magnetron sputtering parameters for YIG films

Material	Argon flow	Deposition power	Target-substrate distance	Argon pressure
YIG	50 sccm	100 W	4.6 cm	3.10^{-2} mbar

These deposition conditions allow obtaining, on alumina substrate YIG films, thicknesses range from 1 to 18 µm, this thickness depends on the duration of the deposit. After deposition, the layers obtained are amorphous and therefore not magnetic. To obtain magnetic properties, YIG films have to be annealed at 740 °C for 2 hours. This annealing is performed in an oven allowing both slow rise and fall times (several hours) to reduce the risk of cracking due to thermal stresses. Morphological, crystallographic and magnetic characterizations of the obtained YIG films are then done.

The thickness of the layer is measured by using a profilometer while images obtained by a Scanning Electron Microscope (SEM) permit to check the quality of the films surface [20]. The crystallographic characterization of YIG layers is obtained by X-ray diffraction (XRD). This method allows identifying the different crystalline phases of the deposited layers but also their concentrations. Figure 6 shows the X-ray pattern of a YIG film having a thickness of 12.4 µm and annealed at 740 °C for 2 hours. The XRD pattern shows that annealed films are pure phase; with significant peaks being indexed with reference card JCPDS 43-0507 of YIG.

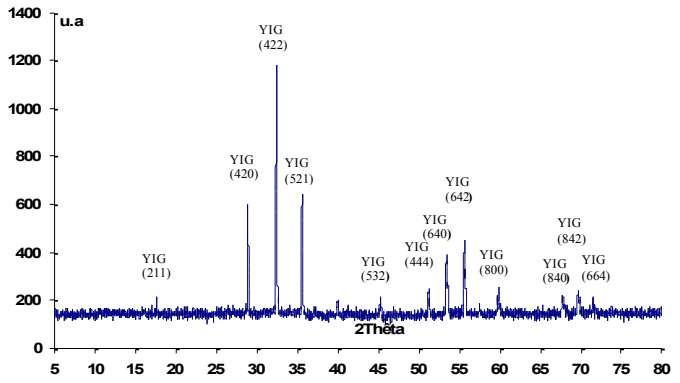

Figure 3: X-ray pattern of YIG film having a thickness of 12.4 µm and annealed at 740 °C for 2 hours.

Finally, the magnetic characterization of the deposited YIG film using the Vibrating Sample Magnetometer (VSM) allows highlighting its magnetic properties.
We have obtained a saturation magnetization of 110 mT and a coercive field of 1.56 kA/m. The saturation magnetization is lower than the bulk material one (175 mT) [21-22] . The coercive field depends on the YIG grain size. So the hysteresis cycle is a soft material cycle. The difference between fig 4.a and 4.b is due to the shape effect.

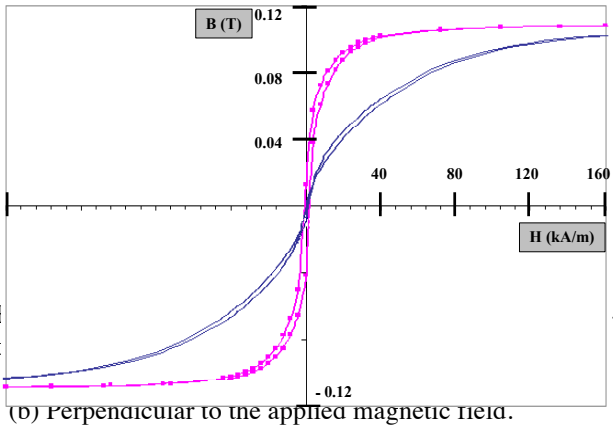

µm

(b) Perpendicular to the applied magnetic field.

3.2. Deposition of the copper film, photolithography and wet etching to obtain the final pattern of the spiral inductor

After the characterization of the deposited YIG thin film, we deposit a copper layer whose thickness is chosen according to the desired application (usually between 1 and 20 µm). The conductive material (copper); deposited by RF sputtering, has been chosen for its high electrical conductivity. For this reason, we have measured by Van der Paw method, the resistivity of the deposited copper film of 5 µm thick. We have measured a resistivity of 2.6×10^{-8} Ω m that is slightly higher than the resistivity of bulk copper (1.7×10^{-8} Ω m).

The realization of the spiral shape is obtained in a clean room by the conventional photolithography technique that can be summarized succinctly as follow:
- Deposition of a photoresist by spin coating (SPR 505).
- Annealing at 110 °C using a hot plate for 90 s.
- UV exposure during 12 s.
- Second annealing at 110°C using an oven for 90 s.
- Revelation and final annealing at 110 °C using an oven for 4mn.

This is followed by wet etching in a solution of ferric chloride at 30 °C. The etching time depends on the concentration of ferric chloride, the temperature of the solution and the thickness of the deposited layer. The etching is generally performed in less than 1 minute.

4. Fabrication of the integrated inductor with thick magnetic film

The deposition of magnetic layers by RF magnetron sputtering has important advantages concerning the purity of the obtained thin films and the high deposition rate compared to the other techniques. But this deposition rate remains low to obtain thick magnetic layers during a reasonable time (a few hundredths of microns in order to have significant effects on the inductance value). On the other hand it is quite unrealistic to expect obtaining such thick layers.
To use thicknesses between 50 and 500 µm, the implementation of commercial substrates was chosen. In this section we present the process of manufacturing of inductors on thick layers obtained by micromachining.
The fabrication process includes the following main steps:

- Preparation of YIG substrate by micromachining (grinding and polishing).
- Deposition of copper layer on the YIG substrate by RF magnetron sputtering.
- Photolithography and wet etching necessary to obtain the pattern of the spiral inductor.
- And finally, the wire bonding for the terminal connections.

4.1. Preparation of YIG substrate by micromachining

We wish obtaining a thick film of YIG (substrate of several tens of microns to several hundred microns) from a bulk plate having a thickness of about 1 mm. As the YIG (ferrite) is brittle to be manipulated by micromachining; the ferrite plate is stuck on a glass substrate. For this sticking, two types of glue are used depending if the YIG plate will be peeled off from the glass substrate or not. We proceed then to the grinding of the YIG plate in order to obtain the desired thickness. The final thickness could be controlled with a high accuracy (a few microns).
The substrate roughness has an influence on the electromagnetic properties, but also on the mechanical

properties of the components [20]. The effect of roughness on performance of biosensors was fully addressed for plane biosensors and gratings [23]. After grinding, the samples present a mediocre surface state. The measured roughness R_a (arithmetic mean value) ranges from 200 nm to 500 nm. For this reason the grinding is then followed by polishing that permits to obtain a better surface quality sufficient to achieve planar patterns by photolithography. A high roughness allows a very good adhesion of the conductive layer to be deposited, but this high adhesion, introduce difficulties in the step of etching. To simplify the manufacturing process by avoiding the deposition with high adhesion, a roughness of several tens of nm is a compromise between adherence and quality of etching. The grinding is performed with a machine having ¼ µm diamond suspension. A period of grinding of about 20mn is enough to obtain the desired roughness.

4.2. Morphological and magnetic characterization of the YIG substrate

After manufacturing the YIG substrate we have done the morphological characterization by studying the roughness of the sample surface. Figure 5 illustrates two types of roughness measurements of the surface obtained before polishing. The first one corresponds to a measurement using a profilometer and the second one have been performed by Atomic Force Microscopy (AFM).

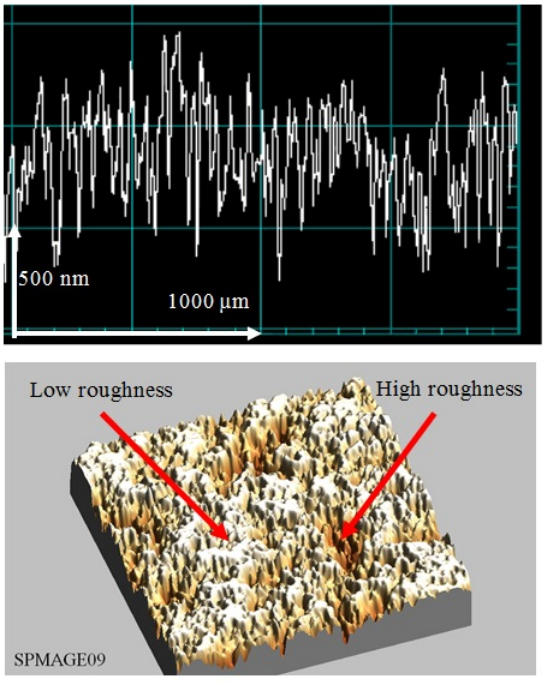

Figure 5: Profile of the sample surface before polishing: a) with profilometer, b) with AFM

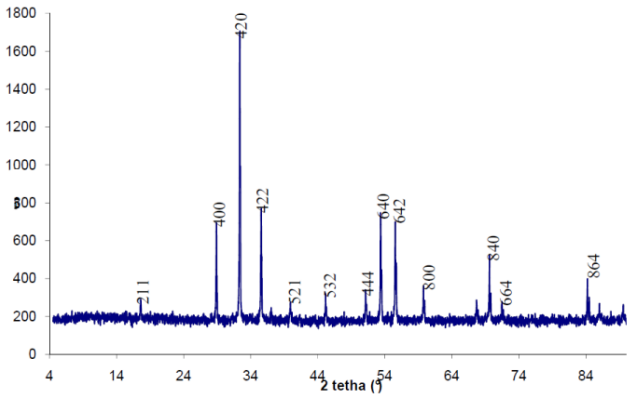

Figure 6: X-ray diffraction pattern for a thick layer obtained by micromachining

Typically, after polishing the average of the roughness Ra is close to 80 nm. This value is a good compromise between adhesion of the layer and quality of wet etching. We have also verified the crystallographic structure of the material by performing a characterization by X-ray diffraction (fig. 6). The diffraction planes; compared with the reference file JCPDS 43-0507 of YIG, show that the peaks correspond to $Y_3Fe_5O_{12}$. One can observe a good agreement with the reference file, because, for example the peak of maximum intensity is obtained for the plane [420] corresponding to an angle of 32.3 ° as in the reference file.

To perform the magnetic characterization of the micro-machined substrate of YIG, we have used the VSM technique. Figure 7 shows the hysteresis curves obtained by VSM for a thick layer of YIG prepared by micromachining. The saturation magnetization of thick layer is about 175 mT and the coercive force is about 0.5 kA/m. This value is very closed to the saturation magnetization of the bulk YIG. A shape effect is observed, corresponding to the magnetic applied field during the measurement.

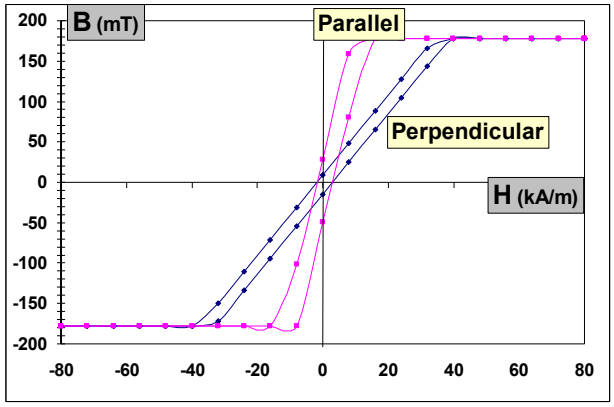

Figure 7: VSM hysteresis curves of a YIG substrate for parallel and perpendicular applied field

4.3. Deposition of the copper micro-inductor in its spiral shape

After these characterizations of the micro-machined YIG substrate a spiral micro-inductor of copper have been deposed on it, as in the section 3.2. To connect by a conducting wire, the central end of the spiral with the terminal connection of the inductor, we have used the bonding technique. Figure 8 shows the manufactured spiral micro-inductor with thick YIG layer.

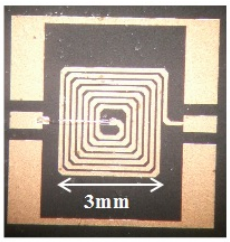

Figure 8: Photo of the manufactured spiral micro-inductor with thick YIG layer

5. Equipment for inductance measurement

The measurement of the inductance of the manufactured micro-integrated inductors is a very important step of our study. This inductance has been measured as a function of the thickness of the magnetic material and of the frequency. Two types of equipment have been used depending on the frequency range.

5.1. Low frequency equipment

For low frequency, we have used equipment composed of a LCR-meter (HP 4284A) and a four probe test bench. The LCR-meter is an impedance bridge permitting to measure with accuracy the real and the imaginary parts of the impedance or the admittance of the Device Under Test (DUT). It permits, with the four probe test bench, to eliminate the effect of parasitical impedances and connection cables by using the SHORT correction.

5.2. High frequency equipment

For high frequency, we have used an equipment composed of a vector network analyzer of Agilent N5230A associated with a high frequency probing tester. It permits to measure dispersion parameters in two ports with OSL calibration (Open-Short-Load) permitting to correct errors due to cables, probes and connections. The conversion of dispersion parameters into inductance is done using RL series in parallel with the parasitic capacitance C model.

6. Results and discussion

6.1. Micro-integrated inductor with YIG layer

The measured inductance of the manufactured spiral integrated inductor without magnetic core is about 100nF. The inductance is multiplied by 1.14 when the same inductor is deposited on a thin YIG layer of thickness about 17 µm. This increasing of the inductance remains modest because the magnetic field lines are not well guided by the magnetic thin YIG core. This result justifies the fabrication of the second type of integrated inductor on a micro-machined plate of YIG. In this case and for thick magnetic YIG layers (thickness of few hundreds of microns), the inductance is multiplied by 2 compared to coreless micro-inductor. Figure 9 presents the inductance as a function of thickness for the micro-machined structures at low frequency (1MHz). For these thicknesses, the field lines are well guided by the magnetic material and the maximum measured inductance is two times higher than the micro-inductor without magnetic material. The layer thickness has any influence over 200 µm. The field lines are canalized. The inductance is near of the one obtained by Yaya [24].

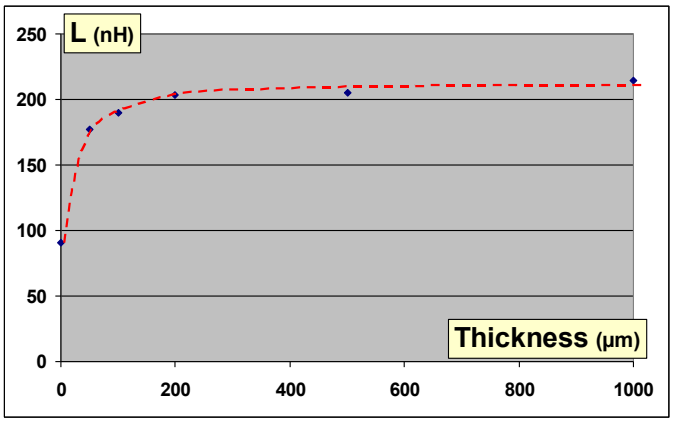

Figure 9: Measured inductance of the integrated inductor deposited on a thick micro-machined layer versus its thickness at low frequency (1MHz)

Figure 10 shows the evolution of the inductance L of structures with and without magnetic material as a function of frequency. In this figure the subscripts of L indicates the thickness of the magnetic material and the type of characterization: measurement “M” or simulation “S”. Thus, “0” indicates a structure without magnetic material, “17” for a micro inductor deposited by RF sputtering on a thin YIG film of thickness equal to 17 µm and “200” for an integrated inductor deposited on a thick layer obtained by micro-machining and having a thickness of 200 µm.
Figure 10 shows that the measured inductance for thick magnetic layer (thickness of 200 µm) decreases when the

frequency increases. This phenomenon could be explained by the fact that the permeability decreases by the increasing of the frequency. Same results are observed for thin magnetic films, but the decreasing of the measured inductance is less noticeable. However, the simulated values of the inductance remain practically constant because the permeability is maintained constant during the simulation for all frequencies [25].

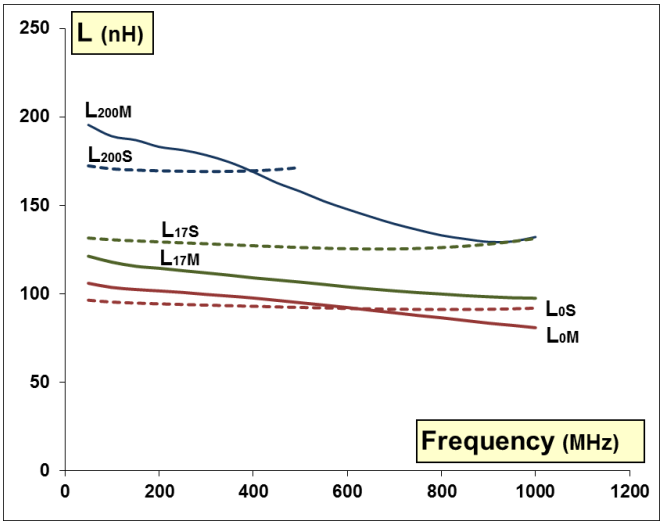

Figure 10: Measured (M) and simulated (S) inductance of the micro-inductor versus frequency for different thicknesses of the magnetic material (0 μm, 17 μm and 200 μm)

By comparing results obtained for thin and thick magnetic layers with the inductance without magnetic material (fig. 10), we noticed that by using the micro-machined thick layer permits to double the value of the inductance as shown in figure 9. However, for thin magnetic films a ratio of 1.14 is obtained. The YIG magnetic permeability decreases with the frequency increasing.

7. Conclusion

In this work, we have manufactured two types of integrated inductor with magnetic material by micromachining for thick layers and by RF sputtering techniques for thin films. The spiral shape of copper was obtained by microelectronics technique. Characterizations obtained at high and low frequencies have to highlight the influence of the magnetic layer thickness on the performance of the inductors. Inductance measurements have shown that magnetic thin films deposited by RF sputtering permit to increase the inductance value, but the effect remains weak; a ratio of 1.14 for a thickness of 17 µm of YIG is obtained by comparison with the coreless micro-inductor. For this reason we have used thick micro machined YIG layers permitting to double the inductance value. This technique of micro-machining is done by gluing, sawing, grinding and polishing of a YIG substrate followed by morphological, crystallographic and magnetic characterizations. We have also compared the measured and simulated results to validate our original techniques of the integrated spiral inductor with thin and thick layers.

References

1. Charles R. Sullivan and Seth R. Sanders. IEEE Transactions on Power Electronics, **11**, 2, 228, (1996)
2. B. Estibals, J.-L. Sanchez, C. Alonso, H. Camon, J.-P. Laur. J3eA, Journal sur l'enseignement des sciences et technologies de l'information et des systèmes, **2**, 2, (2003)
3. J. N. Burghartz, D. C. Edelstein, M. Soytter, H. Ainspan and K. Jenkins, IEEE Journal of Solid-state Circuit, **33**, 12, 2028 (1998).
4. A. Telli, S. Demir and M. Askar.. Proceedings of 11th IEEE International Conference on Electronics, Circuits and Systems, December 2004, ICECS, (2004) p487
5. Jong-Min Lee, Tae-Woo Lee, Sung Ho Park, Byoung-Gue Min, Moon Pyung Park, Kyung-Ho Lee and In-Hoon Choi, Institute of Physics Publishing, Semiconductor Science and Technology, **16**, 2, 66, (2001)
6. Jinwen Zhang, Wai Cheong Hon, Lydia L W Leung, and and K J Chen, Institute of Physics Publishing, Journal of Micromechanics and Microengineering, **15**, 328, (2005)
7. Ming-Chun Hsieh, Yean-Kuen Fang, Chung-Hui Chen, Shuo-Mao Chen and Wen-Kuan Yeh, IEEE Transactions on Electron Devices, **51**, 3, 324 (2004)
8. X.L Tang, H.W Zhang, H. Su, H. Shi and X.D. Jiang.. JMMM, **293**, 812 (2005)
9. Yong-Kyu Yoon and Mark G. Allen, Institute of Physics Publishing, Journal of Micromechanics and Microengineering, **15**, 1317, (2005)
10. S. Kirouane, D. Vincent, E. Vernet, O. Zahwe, B. Payet-Gervy and A. Chaabi, Eur. Phys. J. Appl. Phys. **57**, 10602 (2012)
11. P. M. Trabulo, D. A. Durães, P. M. Mendes, P. Garrido and J.H. Correia, Materials Science Forum, **455**, 116, (2004)
12. Jan Van Heze. *Accurate modelling of spiral inductors on silicon for wireless FFIC designs* [on line]. TechOnLine. November 2001.
13. Mina Rais-Zadeh and Farrokh Ayazi, Institute of Physics Publishing, Journal of Micromechanics and Microengineering, **15**, 2105 (2005)
14. Tingrui Pan, Antonio Baldi, Emile Davies-Venn Rhonda F Drayton and Babak Ziaie, Institute of Physics

Publishing, Journal of Micromechanics and Microengineering, **15**, 849, (2005)
15. R. Murphy-Arteaga, J. Huerta-Chua, A. Diaz-Sanchez, A. Torres-Jacome, W. Calleja-Arriaga, and M. Landa-Vázquez, Microelectronics Reliability, **43**, 195, (2003)
16. Choon Beng Sia, Kiat Seng Yeo, Manh Anh Do and Jian-Guo Ma, IEEE Transactions on Semiconductor Manufacturing, **16**, 2, 220, (2003)
17. Jan Van Hese. *Design and simulation of spiral inductors on silicon substrates* [on line]. ChipCenter Questionlink. 2001, pp.1-2.
18. B. Abdel Samad, M.-F. Blanc-Mignon, M. Roumie, A. Siblini, J. P. Chatelon and M. Korek**,** Eur. Phys. J. Appl. Phys. **50,** 1, 10502**,** (2010)
19. S. Capraro, T. Boudiar, T. Rouiller, J.P. Chatelon, B. Bayard, M. Le Berre, B. Payet-Gervy, M.F. Blanc-Mignon and J.J. Rousseau, Microwave and Optical Technology Letters, **42,** 6, 470 (2004)
20. I. Khalil, A. Siblini, J.P. Chatelon, M.F. Blanc-Mignon, and J.J. Rousseau, Phys. Status Solidi A, **208**, 7, 1678, (2011)
21 Landolt-Börnstein. « Numerical data and functional relationships in science and garnets technology », v.12 « Magnetic and other properties of oxides and related compounds and perovskites », K.-H. Hellwege (ed.), Springer-Verlag Berlin, p. 500, 1978.
22 N.B. Ibrahim, C. Edwards, S.B. Palmer. J. Magn. Magn. Mater, 220, p. 183-194, 2000.
23. Sameh Kessentini, Dominique Barchiesi, Advanced Electromagnetics, vol.1, n°2, (2012) 41-47
24. Dagal Yaya, Désiré Allassem, Mahamoud Youssouf, Ali Siblini, Jean Pierre Chatelon and Jean Jacques, Rousseau, Advanced Electromagnetics, vol.1, n°2, (2012) 58-63
25. Adoum Kriga, Désiré Allassem, Malloum Soultan, J.P. Chatelon, A. Siblini, B. Allard, J.J Rousseau, JMMM, **324**, 14, 2227, (2012)